ABSTRACT

Pamela Ross: Time-course Comparison of Xenobiotic Activators of CAR and PPAR-alpha in Mouse Liver
(Under the direction of Ivan Rusyn, M.D., Ph.D.)

Constitutive androstane receptor (CAR) and Peroxisome Proliferator Activated-Receptor (PPAR)-alpha are two nuclear receptors of interest which are activated by phenobarbital (PB) and WY-14,643 (WY), respectively. In order to capture the global transcriptional changes that result from activation of these nuclear receptors over a time course, microarray technology was used to establish fingerprints of gene expression in the mouse liver. First, we examined differences in basal expression between wild-type and *Car*-null mice and found 14 significantly differentially expressed genes. Next, Extraction of Differential Gene Expression (EDGE) algorithm was used to identify genes that changed with regards to both time and treatment, and these genes were submitted to the Gene Ontology (GO) Database to identify significantly enriched biological pathways. While several pathways dealing with cellular proliferation and metabolism were identified in the wild-type, no significant pathways were found to change over time in the *Car*-nulls. Next, to determine commonalities and differences in the temporal response to activators of CAR and PPAR-alpha, gene expression signatures from wild-type mice treated with PB or WY were compared. Similar pathways were affected by both compounds, but the regulation of these genes showed differences over time. This study establishes common fingerprints of

exposure to activators of CAR and PPAR-alpha in rodent liver and demonstrates the changes that correlate with the presence or absence of a corresponding nuclear receptor.

ACKNOWLEDGEMENTS

I would like to sincerely thank my advisor, Dr. Ivan Rusyn, for guidance during both my undergraduate and graduate careers and for hiring me as a work-study student as a freshman. I definitely would not have accomplished my academic and scientific goals without his mentorship. I would also like to thank Mrs. Blair Bradford for being my lab mom for the last six years and always encouraging me for every step of my career. I sincerely appreciate former and current lab mates from the Rusyn lab who not only helped with experiments but also provided much-welcomed friendship. Thanks especially to my BFF who provided entertainment and encouragement as my lab mate.

This research was based on previous studies by Dr. Courtney Woods, and data collection was aided by Mrs. Oksana Kosyk and Mrs. Blair Bradford. I also wish to thank Ms. Alison Hege and Mr. Dan Gatti for technical assistance with microarray data analysis and generating figures. Lastly, I thank my family and friends who have been supportive for these last two years of graduate school as well as every other endeavor I have undertaken.

TABLE OF CONTENTS

LIST OF TABLES

LIST OF FIGURES

LIST OF ABBREVIATIONS

CAR	constitutive androstane receptor
DBD	DNA binding domain
DWD	distance weighted discrimination
EDGE	extraction of differential gene expression
GO	gene ontology
LBD	ligand-binding domain
NR	nuclear receptor
PB	phenobarbital sodium
PPAR	peroxisome proliferator-activated receptor
SAM	significance analysis of microarrays
WY	4-Chloro-6-(2,3-xylidino)-pyrimidynylthioacetic acid
WY-14,643	4-Chloro-6-(2,3-xylidino)-pyrimidynylthioacetic acid

CHAPTER 1

LITERATURE REVIEW

A. Overview of Nuclear Receptors

General structure and function

Nuclear receptors (NRs) are a class of ligand-activated transcription factors found in nearly every species and modulate the expression of myriad genes involved in the cell cycle, xenobiotic metabolism, homeostasis and other important physiological processes; in fact, NRs are the largest family of transcription factors known to regulate gene expression (Urquhart *et al.*, 2007). Ligands of NRs are often small, lipophilic molecules that range from endogenous substances such as fatty acids and steroids to a wide variety of xenobiotics. Since many natural substances act as ligands, the action of NRs in regulating basic physiological processes is vital. Upon ligand-binding with a nuclear receptor, a linear series of events occurs which ultimately results in the up- or down-regulation of specific target genes. Thus, the effect of xenobiotic stressors on physiological processes modulated by NRs is also important to study.

Quite surprisingly, over 270 genes encoding NRs have been identified in the nematode *C. elegans* whereas only 21 were found in *Drosophila melanogaster*. An examination of the rat, mouse, and human genomes revealed 47, 49, and 48 NR genes, respectively. Additionally, one aberrant NR gene in each of the mouse and human genomes

was also identified (Zhang *et al.*, 2004). The presence of NRs across many different species highlights their evolutionary importance in the regulation of biological processes.

The nuclear receptor super-family shares a common general structure consisting of an N-terminal sequence with activation functions, DNA-binding domain (DBD), hinge region, and ligand-binding domain (LBD). The highly conserved DNA-binding domain and the ligand-binding domain serve as the distinguishing features of NRs, although subfamily 0 consists of members who lack either a LBD or DBD (Zhang *et al.*, 2004). In order to create a standardized classification of nuclear receptors, the Nuclear Receptors Nomenclature Committee established seven subfamilies (0-6) distinguished by their amino acid sequence similarity (Nuclear Receptors Nomenclature Committee, 1999). Nuclear receptor names are designated by the letters NR, subfamily (Arabic numeral), group (alphabetical letter), and gene (Arabic numeral), but also have more commonly used names (Table 1.1). Historically, NRs have also been grouped into three main classes based on their mechanism of action: steroid hormone receptors which form homodimers, thyroid-like receptors which form a heterodimer with retinoid x receptor (RXR), and "orphan" receptors with no known endogenous ligands.

Mechanisms of activation

Without the presence of a ligand, most NRs are inactive and may reside either in the cytoplasm bound to chaperone proteins or in the nucleus (Aranda *et al.*, 2001). One exception includes the constitutive androstane receptor (CAR) which is constitutively active, but its endogenous ligands androstanol and androstenol serve as inverse agonists which inhibit activity by causing coactivator dissociation (Echchgadda *et al.*, 2007). Usually, ligand-

binding leads to the dissociation of chaperone co-repressor proteins from the NR allowing translocation of the NR-ligand complex into the nucleus. There, most NRs bind to a dimerization partner and may form a heterodimer with retinoid x receptor (RXR) or a homodimer (e.g., estrogen receptor, ER); however, it can also form a monomeric complex (Gronemeyer *et al.*, 2004). Recruitment of co-activator proteins occurs in the nucleus, and the complex is able to recognize a specific DNA response element and subsequently modulate transcription of downstream target genes.

Although not a member of the nuclear receptor super-family, the aryl hydrocarbon receptor (AhR) of the Per-Arnt-Sim (PAS) family of transcription factors shares similar features of activation. AhR ligands such as polycyclic aromatic hydrocarbons and halogenated aromatic hydrocarbons trigger the dimerization of AhR to the AhR nuclear translocator (ARNT) which recognizes helix-loop-helix and PAS binding domains on DNA and leads to transcription of target genes CYP1A1, CYP1A2, CYP1B1, and phase II metabolism genes (Levine *et al.*, 2001).

Role in xenobiotic metabolism

Most notably, nuclear receptors have been shown to induce phase I (e.g., cytochrome P450s) and phase II (e.g., sulfotransferases, glutathione-s-transferases) metabolizing enzymes as well as various transporter genes. These genes are important for the biotransformation and clearance of harmful xenobiotics that may be taken up by the body; however, bioactivation of these compounds may also produce a toxic effect. Another important factor is the broad ligand specificity of some nuclear receptors that make them ideal for xenobiotic sensing. A prime example is pregnane X receptor which has a relatively

large ligand-binding pocket, making it a promiscuous receptor for ligands with diverse structures (Timsit *et al.*, 2007).

Because of their role in mediating cellular metabolic processes and ability to produce pleiotropic effects, nuclear receptors have become an attractive target for pharmaceutical development. This feature has been exploited by cholesterol-lowering fibrate drugs that target peroxisome proliferator-activated receptor-alpha (PPARα) and diabetes drugs which target peroxisome proliferator-activated receptor-gamma (PPARγ) (Gonzalez *et al.*, 2008). It has been estimated that nearly 13% of all FDA-approved drugs target nuclear receptors as its mechanism of therapeutic action. This data is based on 1,357 dosed components from greater than 20,000 approved products as of December 2005 (Overington *et al.*, 2006). Targeting NRs for therapeutic purposes is the ideal goal, but activation of NRs may also be important in disease states such as cancer.

Mode of action in carcinogenesis

One of the accepted paradigms for the induction of cancer is a multi-step process in which an initiating event occurs, followed by progression, irreversible promotion, and finally, carcinogenesis. The initiating event may be caused by two different modes of action: genotoxic or non-genotoxic. Genotoxic events directly damage DNA through processes such as induction of strand breaks or formation of adducts while non-genotoxic mechanisms cause indirect damage through oxidative stress, activation of pro-inflammatory pathways, increased cellular proliferation, inhibition of programmed cell death (apoptosis), or other pathways. Nuclear receptors have been implicated to play a role in cancer by

acting through non-genotoxic modes of action, although the exact mechanisms of action are not clearly distinguished.

One of the non-genotoxic processes modulated by nuclear receptors is the induction of cell cycle genes and promotion of cellular proliferation. Increased cell proliferation shortens the time allowed for the cells' checkpoint machinery to work properly, and the possibility of coding errors is greater. Additionally, clonal expansion of a mutated cell could eventually lead to irreversible progression and cancer once an initiating event occurs. Similarly, the inhibition of apoptosis will result in an increased population of abnormal cells which have the ability to proliferate (Cheung *et al.*, 2006). Another possible non-genotoxic mechanism of action through which nuclear receptors act is the generation of reactive oxygen species. An accumulation of reactive oxygen species promotes increased number of DNA lesions that may lead to mutations which may then lead to cancer. Since it is known that nuclear receptors often induce P450 enzymes, chronic induction of these enzymes may generate reactive oxygen species as a by-product of the oxidation reactions which they catalyze (Gonzalez, 2005). Possible mechanisms are still under debate and continue to be researched in order to elucidate the role of NRs in carcinogenesis.

Genomic profiling of nuclear receptors

Microarray technology allows for the simultaneous measurement of thousands of transcripts in the genome; consequently, it is a highly useful means of examining transcriptional changes elicited by activated NRs. A recent review by Woods et al. gives a comprehensive overview of gene expression experiments on nuclear-receptor mediated toxicity that have been conducted through the time of publication (2007a). In our

experiments, we performed microarrays on activated nuclear receptors in rodents *in vivo* in order to gain insight into the global transcriptional changes that occur in a biologically relevant model. We also highlight the importance of a time-course because many of the changes elicited by activated NRs are dynamic, and a single time-point may not clearly depict the entire range of processes that occur. This may also be important in risk assessments which seek to identify early changes caused by toxicants or xenobiotics that may cause cancer at chronic time-points.

B. Constitutive Androstane Receptor (CAR)

Once described as an "orphan" nuclear receptor without a known cognate ligand, the constitutive androstane receptor (CAR, NR1I3) has now been associated with the endogenous ligands androstanol and androstenol (Forman *et al.*, 1998). When CAR was first discovered, it was considered a peculiar NR because of its constitutive activity; however, this feature is now accepted as common in many orphan receptors. CAR is also unique because its endogenous ligands are not activators, but rather act as inverse agonists which repress its basal activity. In contrast, a wide variety of substrates have been shown to be CAR agonists including phenobarbital, 5β-pregnane-3,20-dione, and phenytoin (Tien *et al.*, 2006;Timsit *et al.*, 2007). Since CAR has relatively broad ligand specificity, and metabolizing enzymes are upregulated as a result of its activation, it has been termed a "xenosensor" (Timsit *et al.*, 2007).

Interestingly, the only chemical which has demonstrated direct binding to mouse CAR is the synthetic ligand 1,4-bis[2-(3,5-dichloropyridyloxy)]benzene (TCPOBOP) while the compound 6-(4-chlorophenyl)imidazo[2,1-*b*][1,3]thiazole-5-carbaldehyde *O*-(3,4-

dichlorobenzyl)oxime (CITCO) specifically binds to human CAR (Tzameli *et al.*, 2000;Maglich *et al.*, 2003;Timsit *et al.*, 2007). This implies that many CAR activators work through an unknown signaling mechanism that does not require direct binding to stimulate translocation to the nucleus. It is hypothesized that a phosphorylation event is necessary for the translocation of the nuclear receptor complex to the nucleus (Yoshinari *et al.*, 2003). Inhibitor studies demonstrated that okadaic acid blocks translocation, presumably by blocking the activity of the protein phosphatase PP2A which mediates the dissociation of CAR from its co-chaperone proteins (Kawamoto *et al.*, 1999; Honkakoski *et al.*, 1998). Much study has been dedicated to the discovery of triggers for nuclear translocation, and it is possible that CAR localization to the cell membrane may play a role in signaling (Koike *et al.*, 2005; Timsit *et al.*, 2007).

Upon entering the nucleus, CAR forms a heterodimer with retinoid x receptor (RXR) and binds to specific promoter elements upstream of target genes including the phenobarbital response enhancer module (PBREM) upstream of CYP2B and the xenobiotic response enhancer module (XREM) upstream of CYP3A. Other target genes of CAR include cytochrome P450s (CYPs), sulfotransferases (SULTs), glutathione-s-transferases (GSTs), and organic ion transporters (OATs). In the mouse, CAR induces transcription of Cyp2b10, Cyp3a11, Cyp2a4 while in the human, CYP2B6, CYP3A4, CYP2C, and CYP2H are induced (Zelko *et al.*, 2000). It is possible that the induction of these phase I enzymes may be rate-limited by the presence of RXR. It has been shown that administration of 9-cis-retinoic acid, a known substrate of RXR, reduced transcription of Cyp2b10 in mice, presumably by reducing the available pool of RXR available to form a heterodimer (Kakizaki *et al.*, 2002).

Phase II enzymes induced by CAR include GSTT1 and SULT1A, and transporter genes include bile salt export pump (BSEP), organic ion transporter 2(OATP2), and multidrug resistance-associated protein 3 (MRP3) (Tien *et al.*, 2006). The coordinate upregulation of these genes is important for the metabolism and excretion of xenobiotics.

Phenobarbital (PB) is a prototypical activator of mouse CAR that does not exhibit direct binding. PB and PB-like compounds had long been observed to induce microsomal enzyme systems, but it was not until the discovery of the CAR gene by Negishi's group that the mode of action was uncovered. The exact mechanism of PB-induced CAR translocation is not yet fully characterized, but a recent study implicates PPP1R16A, a subunit of protein phosphatase 1 beta, as a potential cell membrane mediator (Sueyoshi *et al.*, 2008). Acute effects of phenobarbital administration include increase in the size and number of hepatocytes, and overall liver enlargement (hepatomegaly). Chronic administration of PB has also been shown to reduce triglycerides and increase sensitivity to insulin. Additionally, phenobarbital is a liver tumor promoter in rodents when given chronically.

It is thought that PB works through a non-genotoxic carcinogenic mode of action. Experiments with *Car*-knockouts demonstrate that *Car* is critical for tumor promotion by PB in mice (Yamamoto *et al.*, 2004). The effect of long-term administration of phenobarbital in humans, though, is not clear, and the International Agency for Research on Cancer (IARC) has classified PB as a Group 2B carcinogen or "possibly carcinogenic to humans" (International Agency for Research on Cancer, 2001). There is approximately 72% and 88% sequence concordance of the ligand and DNA binding domains, respectively, between mouse and human CAR, so this may account for some species differences (Timsit *et al.*,

2007). Microarray experiments may help elucidate the non-genotoxic mechanisms through which PB acts. Indeed, many studies have been conducted with PB and PB-like compounds which confirm the role of CAR in activating xenobiotic metabolism genes (Maglich *et al.*, 2002;Ueda *et al.*, 2002; Wei *et al.*, 2000).

C. Peroxisome Proliferator-Activated Receptor-alpha (PPARα)

The peroxisome proliferator-activated receptor (PPAR) family consists of three members: PPARα, PPARβ, and PPARγ. As its name implies, peroxisome proliferators are the class of compounds which serve as the cognate ligands for PPAR. Peroxisome proliferators have the capacity to increase both the size and number of peroxisomes within the hepatocyte of rats and mice. These organelles are instrumental in the beta oxidation of fatty acids and cholesterol synthesis. Although PPARβ and PPARγ are important to study, we chose to concentrate on PPARα because it is the only isoform known to play a role in carcinogenesis (Gonzalez *et al.*, 2008).

Like CAR, PPARα (NR1C1) is highly expressed in the liver but is also present in extrahepatic tissues including the intestine and kidney. Upon translocation to the nucleus, it heterodimerizes with RXR and binds to a promoter element, specifically peroxisome proliferators response element (PPRE). Peroxisome proliferators induce the transcription of genes that promote beta-oxidation of fatty acids and block the activity of acyl CoA oxidase, one of the primary enzymes needed for cholesterol biosynthesis. For this reason, pharmaceuticals have targeted this nuclear receptor for its ability to modulate fatty acid metabolism.

One of the most commonly used and studied peroxisome proliferators is 4-Chloro-6-(2,3-xylidino)-pyrimidynylthioacetic acid (WY-14,643). WY-14,643 has been shown to be predominantly PPARα-specific although some reports of PPARγ activation have also been observed. It is a potent compound and a strong mitogen known for its ability to modulate cell cycle genes. Like phenobarbital, WY causes gross changes in liver including hepatomegaly, hepatocyte hyperplasia and hypertrophy. Peroxisome proliferators such as WY are a well-known class of non-genotoxic rodent hepatocarcinogens that work through PPARα (Reddy *et al.*, 1979). The mechanism of action is not clear but thought to involve an increase in cell proliferation, production of proinflammatory cytokines, and inhibition of apoptosis (Peters *et al.*, 1997;Gonzalez *et al.*, 2008). It is important to note that species differences exist in the strength of expression of PPAR. Palmer et al. (1998) found that human PPARα mRNA is expressed at levels $1/10^{th}$ that of mouse isoforms, implicating a less-important role in mediating carcinogenesis. In fact, a transgenic mouse model of humanized PPAR-alpha only exhibited 5% tumor incidence when given WY-14,643 chronically as compared to 71% of WY-treated wild-type mice (Morimura *et al.*, 2006). An extensive microarray time-course study has previously been conducted in our laboratory that shows temporal and dose-dependent gene expressionc hanges in response to WY-14,643 in wild-type mice (C57Bl/6J) (Woods *et al.*, 2007b). A comparison of the pathways activated by PB through CAR and WY through PPAR-alpha will be examined in order to delineate the changes that occur through these nuclear receptors.

Table 1.1 Nomenclature for nuclear receptors and common names.

Subfamily & Group	Gene Name	Common Name
1A	NR1A1	Thyroid-hormone receptor-alpha
	NR1A2	Thyroid-hormone receptor-beta
1B	NR1B1	All-*trans* Retinoic Acid Receptor-alpha
	NR1B2	All-*trans* Retinoic Acid Receptor-beta
	NR1B3	All-*trans* Retinoic Acid Receptor-gamma
1C	NR1C1	Peroxisome Proliferator-Activated Receptor-alpha
	NR1C2	Peroxisome Proliferator-Activated Receptor-beta
	NR1C3	Peroxisome Proliferator-Activated Receptor-gamma
1D	NR1D1	REV-ERB-alpha
	NR1D2	REV-ERB-beta
	NR1D3	Ecdysone-inducible Gene E75 (Drosophila)
1E	NR1E1	Eip78C Ecdysone-induced protein 78C, DR-78
1F	NR1F1	RAR-related Orphan Receptor-alpha
	NR1F2	RAR-related Orphan Receptor -beta
	NR1F3	RAR-related Orphan Receptor -gamma
	NR1F4	Hormone receptor-like in 46, HR3, DHR
1G	NR1G1	CNR14
1H	NR1H1	Ecdysone receptor, ECR
	NR1H2	Liver X Receptor-beta
	NR1H3	Liver X Receptor-alpha
	NR1H4	Farnesoid X Receptor
1I	NR1I1	Vitamin D Receptor
	NR1I2	Pregnane X Receptor, Steroid X Receptor
	NR1I3	Constitutive Androstane Receptor-alpha, MB67
	NR1I4	Constitutive Androstane Receptor-beta
1J	NR1J1	Hormone receptor-like in 96, DHR96
1K	NR1K1	NR1 Thyroid hormone-like, NHR1
2A	NR2A1	Hepatocyte nuclear factor 4-alpha
	NRK2A2	Hepatocyte nuclear factor 4-gamma
	NR2A3	Hepatocyte nuclear factor 4-beta
	NR2A4	Hepatocyte nuclear factor 4-delta
2B	NR2B1	Retinoid X Receptor-alpha
	NR2B2	Retinoid X Recpetor-beta
	NR2B3	Retinoid X Receptor-gamma
	NR2B4	Ultraspiracle
2C	NR2C1	Testicular Receptor 2
	NR2C2	Testicular Receptor 4
2D	NR2D1	DHR78

Table 1.1 (continued) Nomenclature for nuclear receptors and common names

Subfamily & Group	Gene Name	Common Name
2E	NR2E1	TLL
	NR2E2	Tailless
2F	NR2F1	COUP-TFI
	NR2F2	COUP-TFII
	NR2F3	COUP-TF
	NR2F4	COUP-TFIII
	NR2F5	SVP46
	NR2F6	EAR2
3A	NR3A1	Estrogen Receptor-alpha
	NR3A2	Estrogen Receptor-beta
3B	NR3B1	Estrogen-Related Receptor-alpha
	NR3B2	Estrogen-Related Receptor-beta
3C	NR3C1	Glucocorticoid Receptor, GR
	NR3C2	Mineralocorticoid Receptor, MR
	NR3C3	Progesterone Receptor, PR
	NR3C4	Androgen Receptor, AR
4A	NR4A1	Nerve Growth Factor IB, NGFIB
	NR4A2	Nuclear Receptor Related 1, NURR
	NR4A3	Neuron-derived Orphan Receptor 1, NOR1
	NR4A4	Hormone receptor-like in 38, DHR38
5A	NR5A1	Steriodogenic Factor 1, SF1
	NR5A2	Liver Receptor Homolog-1, LRH1
	NR5A3	FTZ-F1
5B	NR5B1	DHR39
6A	NR6A1	Germ Cell Nuclear Factor
0A	NR0A1	KNI
	NR0A2	KNRL
	NR0A3	EGON
	NR0A4	ODR7
	NR0A5	Trithorax
0B	NR0B1	X-linked orphan receptor, DAX1
	NR0B2	SHP

CHAPTER 2

INTRODUCTION

Nuclear receptors have been a topic of interest due to their important role in cellular signalling and homeostasis. They are the largest known family of transcription factors that function as modulators of tissue gene expression (Urquhart *et al.*, 2007). This also has far-reaching impacts because xenobiotics may serve as ligands for these transcription factors and induce changes in physiological processes. Induction of genes could possibly result in adverse disease states, most notably, cancer. Activation of nuclear receptors CAR and PPARα have already been implicated as the mediators responsible for non-genotoxic modes of rodent hepatocarcinogenesis, although the relevance in humans still remains elusive.

Here, we compared global transcriptional changes in response to activators of CAR and PPAR-alpha in mouse liver over a time-course. We hypothesize that the initial transcriptional responses to the xenobiotic activators PB and WY-14,643 will be different because two different nuclear receptors are activated (CAR versus PPAR-alpha), but at later time-points these pathways will converge because the modes of action of the two chemicals are similar. This study builds on previous work from our laboratory which elucidated temporal changes gene expression in response to WY-14,643, a specific activator of PPAR-alpha (Woods *et al.*, 2007b). The pathways identified in the WY-14,643 data set were compared to enriched biological pathways in response to Phenbarbital (PB), an activator of

CAR. We emphasize the importance of time-course changes because of the dynamic changes elicited by NRs.

CHAPTER 3

MATERIALS AND METHODS

Chemicals

Phenobarbital sodium was obtained from the National Toxicology Program Repository (Lot 4-58-595). 4-Chloro-6-(2,3-xylidino)-pyrimidynylthioacetic acid (WY-14,643) was obtained from Aldrich (Milwaukee, WI).

Animals, Dosing, and Tissue Collection

Male C57BL/6J mice 6-8weeks old were purchased from Jackson Laboratories (Bar Harbor, ME) and male *Car*-null mice (C57BL/6J background) were developed and bred in-house. Genotypes were confirmed by PCR amplification of purified DNA extracted from tail and then run on a denaturing gel. Animals were housed up to four per cage in ventilated cages with standard bedding. The animal room was kept on a 12-hr light/dark cycle at a temperature of 22 ± 2°C and relative humidity 50 ± 5%. The housing facility was maintained by the UNC Division of Laboratory Animal Medicine, and all care was administered in accordance with regulations set forth by the Institutional Animal Care and Use Committee. Animals had free access to purified water throughout the study and the health status of the animals was monitored every other day. Prior to experiments, animals were allowed to acclimate to the animal facility for at least 24 hours and maintained on standard lab chow diet and purified water *ad libitum*.

Mice were given a single acute dose of 0 (control) or 100 mg/kg phenobarbital sodium in distilled water by oral gavage and sacrificed 1 day post-dosing. For sub-chronic treatments, mice were given 0.085% w/w phenobarbital-containing NIH-07 powdered diet or control NIH-07 powdered diet *ad libitum*. Animals (n=3-4) were sacrificed after 7 or 28 days of dietary treatment. At sacrifice, mice were anesthetized with pentobarbital (100 mg/kg) and following exsanguination, livers were removed and weighed. Sections from the left lateral lobe, median lobe, and ventral lobe were fixed in 10% formalin. A portion of duodenum was also included as a positive control for proliferation markers used in immunohistochemistry. A small section of the left lateral lobe was also placed in a vinyl specimen mold, embedded in Tissue-Tek O. C. T. compound (Sakuar Finetek; Torrance, CA), and frozen to -80°C. Frozen sections were later used for lipid staining. The remaining tissue was sectioned, placed in eppendorf tubes, and snap frozen in liquid nitrogen. These samples were stored at -80°C until assayed.

Studies with WY treatment were conducted with data from a previously published report (Woods *et al.*, 2007b) where C57BL/6J mice were administered an acute dose by a single oral gavage of 0 (control) or 50 mg/kg of WY-14,643 in olive oil and sacrificed at 1 day post-dosing. Sub-chronic doses of WY-14,643 were administered in the diet *ad libitum*. NIH-07 was used as the base for the powdered diet containing either 0% (control) or 0.05% w/w of WY-14,643. Mice (n=3) were sacrificed after either 7 or 28 days of dietary treatment.

Clinical Chemistry

At sacrifice, mice were properly anesthetized with 100 mg/kg pentobarbital solution. Blood was collected from the inferior vena cava, placed in collection tubes and spun at 16000*g* for 20 minutes at room temperature. Serum was collected over ice and stored at -20°C before analysis at the UNC Animal Clinical Chemistry and Gene Expression Core Facility. Clinical chemistries for AST, ALK, and triglycerides were measured with an automated Clinical Chemical Analyzer, Vitro 250 (Ortho-Clinical Diagnostic Inc, Rochester NY).

Measurements for ALT in serum were conducted in-house using a standard kinetic assay to measure the disappearance of NADH. Thermo Trace buffer (Thermo Fisher Scientific, cat # TR71021), normal control (cat # 1902-050), and abnormal control (cat#1902-050) were the reagents used for the assay (Thermo Scientific, Waltham, MA). Thermo Trace buffer and plate reader were warmed to 37 °C. Approximately 20 µL of serum or control was added to each well of a clear, 96- well plate. After equilibrating the plate to 37 °C for 5 minutes, 200 µL of Thermo trace buffer was added to each well and incubated for 30 sec. Results were read in the kinetic mode at a wavelength of 340nm with changes in absorbance recorded at 30 sec intervals for 2-3 minutes.

Proliferating Cell Nuclear Antigen (PCNA) Immunohistochemistry and Quantification

Formalin-fixed, paraffin-embedded liver sections (5 µm) were mounted onto glass slides. Sections were deparaffinized in xylene, rehydrated in a series of graded alcohol concentrations, and placed in PBS with 1% Tween 20. Immunostaining was performed using DAKO EnVision System HRP (Dako Cytomation, Carpinteria, CA) with primary Monoclonal

antibody PCNA (Dako, M0879) diluted in PBS containing 1% bovine serum albumin and incubated overnight at 4°C. Slides were counterstained with hematoxylin (). Quantitative analysis of immunostained liver sections was performed using BIOQUANT software (BIOQUANT Image Analysis, Nashville, TN) by dividing the number of positively stained nuclei to total nuclei within 10 random fields at 200x magnification.

Oil Red O Staining and Quantification

Oil Red O stain was used as a marker for triglycerides and lipids, and all staining was performed by the Animal Histopathology Core Facility, a division of the UNC Lineberger Comprehensive Cancer Center. Frozen sections 5-7 microns thick were mounted onto slides in distilled water and placed into a bath of absolute propylene glycol for 2 minutes. Slides were then immersed in 0.5% Oil Red O solution (0.5g Oil Red O in 100 mL propylene glycol) for one hour, rinsed in 85% propylene glycol for 1 minute, washed with distilled water, and stained with Harris Hematoxylin. After rinsing with distilled water, a 1% lithium carbonate-aqueous solution was applied and followed by three rinses with distilled water. Slides were then dehydrated with serial dilutions of ethanol up to xylene and coverslipped with permount mounting media.

Quantitative analysis of stained liver sections was performed using BIOQUANT software (BIOQUANT Image Analysis, Nashville, TN). The percent area stained was determined by dividing the area of positively stained red droplets to total area of the tissue. This was accomplished by randomly selecting 10 fields on each slide at 200x magnification.

RNA Isolation

Total RNA was isolated from the right lobe of the liver using Qiagen RNeasy Mini Kit (Qiagen, Valencia, CA) according to manufacturer's protocol. Briefly, approximately 30 mg of frozen tissue was immersed in 600 µl of RLT lysis buffer containing 1% β-mercaptoethanol and homogenized using the Ultra-Turrax® T8 homogenizer (IKA, Wilmington, NC). The homogenate was centrifuged at 16000*g* for three minutes. Total RNA was extracted from the resulting lysate (supernatant) by ethanol precipitation then bound to a column membrane, washed, and eluted in RNase-free water. RNA purity and integrity were assessed using RNA 6000 Nano Assay LabChips® (Agilent Technologies, Santa Clara, CA) and analyzed on a 2100 Bioanalyzer (Agilent Technologies, Santa Clara, CA) according to manufacturer's protocol.

cDNA Preparation and Microarray Hybridization

Preparation of cDNA, labeling and hybridizations were performed using reagents from the low RNA input fluorescent linear amplification kit (Agilent Technologies) based on the manufacturer's protocol. A pooled mouse RNA sample (Cogenics, RTP, NC) derived from equal amounts of RNA from kidney, spleen, lung, brain, and liver was used as a reference and prepared in parallel to the samples of interest. Samples were analyzed using an Agilent Mouse Oligo Microarray (~21,000 features, catalog# G4121). The hybridized microarrays were washed and scanned using an Agilent G2565BA scanner. Data were extracted from the scanned image using Agilent Feature Extraction software version 9.1. Raw data is available from the UNC Microarray database (genome.unc.edu).

Microarray Data Analysis

Array quality was assessed by Agilent Feature Extraction software and genes with fewer than 70% present data across all arrays were excluded from further analysis. LOWESS normalization was performed to eliminate dye bias. For a given gene, the Cy5/Cy3 ratios were divided by the average Cy5/Cy3 ratio for their time-matched controls. Missing data points were calculated using K-nearest neighbor imputation method. Average-linkage, hierarchical clustering was performed using Cluster software on median centered (by genes) data and visualization was facilitated by Java Treeview. Batch effects were removed using Partek Genomics Suite in which an ANOVA model was fitted and removed residuals due to batch effects. For analysis comparing gene-by-gene differences in PB versus WY samples, Distance Weighted Discrimination (DWD) was used to combine the two data sets. This method uses a linear discrimination method to classify samples and is beneficial because it avoids data piling (Benito *et al.*, 2004).

Differentially expressed genes were identified using either Significance Analysis of Microarrays (SAM) or EDGE software (Tusher *et al.*, 2001; Leek *et al.*, 2006). SAM was performed in cases where statistical significance across only one variable (strain, time, or treatment) was being assessed. EDGE was used for identifying differentially expressed genes across two or more variables (i.e., time and treatment). Q-values, which represent the false discover rate (FDR) of less than 0.05 for SAM and EDGE were selected as thresholds for differential expression. Once the list of significant genes was generated by EDGE, a t-statistic was calculated for each gene at each treatment/time combination to determine statistical difference between treatment and control expression. For each

treatment/time combination, a list of differentially expressed genes ($p<0.05$) was used for functional analysis and generation of gene networks.

Functional Analysis of Significant Gene Sets

High-Throughput GOMiner was used to determine biological function of differentially expressed genes, in the context of Gene Onotology (GO) (Zeeberg *et al.*, 2005). High-Throughput GOMiner is designed to facilitate pathway mapping in cases when several gene lists are to be analyzed. High-Throughput GOMiner was used for pathway analysis of significant genes lists generated from EDGE time-course analyses. A Q-value, representative of the FDR <0.05 and $P<0.05$ were the basis for statistical significance from this analysis. Finally, gene networks were generated by Ingenuity Pathways Analysis (Ingenuity Systems, Redwood City, CA).

Generation of Gene Networks

Significantly differentially expressed genes by time-point and treatment were uploaded into Ingenuity Pathways Analysis and identified as focus genes. The gene network algorithm identifies "top networks" limited to 35 genes ("network nodes") and creates pathways to maximize connections between the focus genes. Nodes were colored by fold change over control with red indicating upregulation or green indicating down-regulation and intensity of color coinciding with greater fold change of treatment over time-matched control.

CHAPTER 4

RESULTS AND DISCUSSION

Phenotypic changes in mouse liver in response to phenobarbital in Car-wildtype and Car-null

It has been previously shown that phenobarbital elicits pleiotropic effects on the mouse liver including hepatocellular hypertrophy, hyperplasia, and hyper-proliferation of the smooth endoplasmic reticulum (Bell and Michaelopolous 2006). As expected, wild-type phenobarbital-treated animals exhibited a significant increase in liver to body weight ratio at 7 and 28 days in comparison to their time-matched controls whereas no such effect was evident in the *Car*-null (Table 4.1). Examination of hematoxylin and eosin stained sections of wild-type phenobarbital-treated livers showed enlarged hepatocytes at 7 and 28 days. Immunohistochemical staining with Proliferating Nuclear Cell Antigen (PCNA) antibody was used to quantify the number of nuclei in early G1 phase and S phase of the cell cycle. The change in hepatocellular proliferation followed a bell-shaped curve with lower-levels at 1 day followed by a proliferative burst at 7 days which then subsided after 28 days exposure. The increase in nuclear staining of replicating hepatocytes did not reach levels of significance based on Student's t-test between PB-treatment and time-matched control. Clinical chemistry markers for liver injury such as alanine aminotransferase (ALT) did not significantly change with PB-treatment in either the wild-type or *Car*-null animals. There

were also no significant changes in other clinical chemistry markers including aspartate aminotransferase, alkaline phosphatase, and serum triglycerides (data not shown).

Basal differences in gene expression of Car-wildtype and Car-null

One of the data gaps identified in reviewing the research on constitutive androstane receptor is identification of the innate difference in gene expression of the *Car*-wildtype mouse liver versus its corresponding knockout. To our knowledge, other researchers have not presented this data in the current literature, although it has been noted that no overt phenotypes result from the deletion of *Car* (Wei *et al.*, 2000). It is important to examine these differences in order to determine the effects that the genetic background may have on the levels of these genes once *Car* is activated. Here, we compared wild-type C57BL/6 control animals to *Car*-null controls on the same genetic background by using a two-class SAM analysis across all time-points and found 14 unique, differentially expressed genes (Figure 4.1). Of these 14 genes, half are located on the same chromosome as the *Car* gene (chromosome 1) including activating transcription factor 6 (*Atf6*), mannoside acetylglucosaminyltransferase 5 (*Mgat5*), protoporphyrinogen (*Ppox*), cathepsin E (*Ctse*), Purkinje cell protein 4-like (*Pcp4l1*), UDP N acetylglucosamine pyrophosphorylase 1 (*Uap1*), and *1700009P17Rik*. This may indicate that the differential expression of these genes between the wild-type and knockout may be related to the congenic interval carrying *Car* rather than changes in expression attributable to being a *Car*-knockout. In constructing a knockout, there is some carryover between the gene target when back-crossing to the desired genetic background, and this does not have major relevance to innate differences in the wild-type versus knockout.

Those genes not found on the same congenic interval as *Car* include a number of cytochrome P450s (*Cyp2c29, Cyp2c39, Cyp2c37*), interferon-gamma inducible protein 47 (*Ifi47),* lymphocyte antigen 75 (*Ly75*), mixed lineage kinase domain-like (*Mlkl*), and an uncharacterized RIKEN (*583047M02Rik*). Both Cyp2c37 and Cyp2c29 have been shown to be directly regulated by *Car* upon exposure to phenytoin, a PB-like compound (Jackson *et al.*, 2004;Jackson *et al.*, 2006). Cyp2c39 is a liver-specific cytochrome P450 that is involved in the metabolism of retinoic acid, which is a known substrate of CAR (). All of these CYP genes are downregulated in *Car*-null as compared to the wild-type. Similarly, the genes *Ifi47, Ly75, and Mlkl* are all downregulated in the knockout compared to the wild-type. These genes have scarcely been studied, but it is possible that *Ifi47* and *Ly75* may be involved in a defense response signaling under the control of *Car*. More research must be conducted to identify the significance of these genes.

Car-specific transcriptional response over a time-course is evident in wild-type liver in response to phenobarbital

Although previous studies have reported differential gene expression in response to PB at a single time-point, we sought to identify how genes changed over a time-course at early, intermediate, and subchronic time-points. Extraction of Differential Gene Expression algorithm was used to identify genes that varied in response to both time and treatment. Analysis revealed 1855 genes that were significantly different in response to phenobarbital treatment in wild-type mouse liver over 1, 7, and 28 days. Hierarchical clustering of these significant genes and visualization with Java TreeView showed patterns of induction across time-points in response to PB. When these same genes were visualized in the *Car*-null data

set and ordered in the same hierarchy, no distinct patterns of induction were visually evident, indicating a *Car*-specific signature (Figure 4.2A). EDGE analysis performed in the *Car*-null data set produced 16 differentially expressed genes, but no significant pathways were identified from this gene set (data not shown).

A canonical pathway for the activation of CAR was modified from Ingenuity Pathways Analysis and overlayed with expression values given as fold-change over control to show a time-course of the specific genes that were changing in response to PB treatment (Figure 4.2B). These were further divided into phase I, II, and transporter genes. The intensity of the color for up- (red) or down-regulation (green) is based on increasing fold change value. The results showed that different isoforms of CYPs were induced at early versus later time-points. CYP3As were upregulated at 1d, but at 7 and 28d, there was an upregulation of CYP2C. Glutathione-s-transferase was upregulated at 1 and 7d, but downregulated at 28d, possibly returning to steady state. The transporter MRP3 was upregulated continually over the time-course.

Gene-by-gene comparison of time-course responses to PB and WY

EDGE analysis of the WY data set was previously reported by Woods et al. (2007b) and was used as a basis of comparison for the PB data. Since the two sets of experimental arrays were performed in different batches, Distance Weighted Discrimination (DWD) was used as a correction method to account for batch effects between the two microarray data sets (Benito *et al.*, 2004). A heat-map of EDGE significant genes in the wild-type in response to PB was generated. These same genes were identified in the WY data set and ordered in the same hierarchy (Figure 4.3A). Likewise, a heat-map of EDGE significant

genes in the wild-type in response to WY was also generated, and the PB data set was compared to it (Figure 4.3B).

Pathway-level comparison of responses to PB and WY

Significant genes from each separate PB or WY EDGE analysis were submitted to High-Throughput GOMiner to identify enriched biological processes at each timepoint in response to treatment (Figure 4.4). An R script written by Daniel Gatti, M.S. was used to generate a visual representation of the False Discovery Rate (FDR) of each significant biological pathway. Greater intensity of color represents a more significant FDR, and color indicates up- (red) or down-regulation (green) of the pathway. The order of the GO pathways is organized based on GO hierarchy.

From the significant pathways identified by High-Throughput GOMiner, general categories could be inferred including cell proliferation, metabolism, immune response, and other miscellaneous responses. In the cell proliferation block, there appears to be similar upregulation at 7 days PB treatment and 7 and 28 days of WY treatment. The cell proliferation response is not evident at 28 days of PB treatment. This data is consistent with the phenotypic response from the PCNA marker of cell proliferation which shows an elevated response at 7 days and subsides at 28 days. Although we hypothesized that there would be similar pathway induction at later time-points, there was a shift in the significance of the response to PB treatment. In observing changes in metabolism, the inductions of pathways in response to PB or WY treatment were dissimilar. A temporal biphasic response to sterol, lipid, and cholesterol biosynthetic processes was observed in PB treated groups where there was an upregulation at 1d followed by down-regulation at 28d. In contrast,

lipid metabolic processes and fatty acid metabolism were only upregulated following WY treatment at 7 and 28d. Immune response pathways were similarly downregulated in both treatments, but the time-course was different. Complement activation pathways were downregulated at 1d PB treatment whereas downregulation of these pathways in response to WY were observed at 7 and 28d. Other processes such as DNA repair, cell communication, and neurophysiological processes were significant in the WY group at 7 and 28d but not at any time-point in the PB groups.

Specific gene networks show varying patterns of modulation

The pathway-level analysis of the genes changing across the time-course was important to study, but specific gene networks showing patterns of these genes were also examined. Ingenuity Pathways Analysis generated "top networks" from the focus genes that were input from the EDGE analysis. The first top network was the DNA Replication, Recombination, and Repair, Cell Cycle, Cell Death Network. This network showed a smiliar pattern of induction in response to PB at 7 days (Figure 4.5A) and WY-14,643 at 28d (Figure 4.5B). Minichromosome maintenance genes (MCMs) were upregulated in both sets, and these genes are important in DNA replication and cell cycle. Ubiquitin-like, containing PHD and RING finger domains, 1 (UHRF1) is also upregulated in both sets and is a cell cycle checkpoint gene and necessary for liver growth (Sadler *et al.*, 2007).

One of the top networks that showed a divergent pattern was the Cell Death, Organismal Injury and Abnormalities, and Cancer Network in response to PB (Figure 4.5C) and WY (Figure 4.5D) at 28d. Many of the focus genes were upregulated in response to PB whereas these nodes were mostly downregulated in response to WY. For example, CD27,

complement genes, and interleukin genes were upregulated in response to PB but downregulated with WY treatment. This may be indicative of a stronger inflammatory response in the PB treated animals. There may be a dissimilar mode of action or it may point to different non-genotoxic modes of action playing a more important role than others. The 28d subchronic time-point is not long enough for the cancer to be produced, but it is speculated that the general cell machinery would already be activated at this time.

Table 4.1. Phenotypic endpoints in livers of wild-type and *Car*-null mice in response to phenobarbital (PB) treatment. *Indicates value significantly different from time-matched control by Student's t-test, $p<0.05$.

	Car +/+						*Car* -/-					
	1d		7d		28d		1d		7d		28d	
	CON	PB	CON	PB	CON	PB	CON	PB	CON	PB	CON	PB
% Liver to Body Weight	5.2 ± 0.4	5.5 ± 0.1	5.8 ± 0.4	**6.6 ± 0.3***	5.8 ± 0.5	**6.8 ± 0.2***	5.5 ± 0.8	6.0 ± 0.4	5.4 ± 0.2	5.3 ± 0.5	5.6 ± 0.1	5.3 ± 0.2
ALT (U/L)	50.7 ± 11.4	28.5 ± 11.7	33.4 ± 30.8	24.9 ± 7.1	16.3 ± 5.4	36.6 ± 13.6	26.1 ± 13.4	69.8 ± 23.4	16.4 ± 4.4	39.8 ± 18.3	21.1 ± 5.7	39.8 ± 18.3
PCNA (% nuclei stained)	6.2 ± 3.5	6.4 ± 4.1	13.5 ± 3.1	23.6 ± 7.3	10.5 ± 4.4	16.1 ± 5.3	10.1 ± 3.4	12.1 ± 14.1	18.6 ± 3.6	9.3 ± 5.0	10.2 ± 3.9	16.5 ± 6.9
Oil Red O (% area stained)	0.42 ± 0.34	3.32 ± 2.94	0.16 ± 0.15	0.22 ± 0.15	1.34 ± 0.96	1.65 ± 1.54	0.34 ± 0.29	0.73 ± 0.54	1.52 ± 1.01	0.93 ± 0.96	3.43 ± 1.58	1.71 ± 1.57

Figure 4.1. Hierarchical clustering reveals 14 unique, differentially expressed genes between *Car* WT and KO mice. Prior to performing time-matched control normalization, an unpaired, two-class SAM analysis was conducted to basal differences in gene expression between *Car* WT and KO mice across all time points.

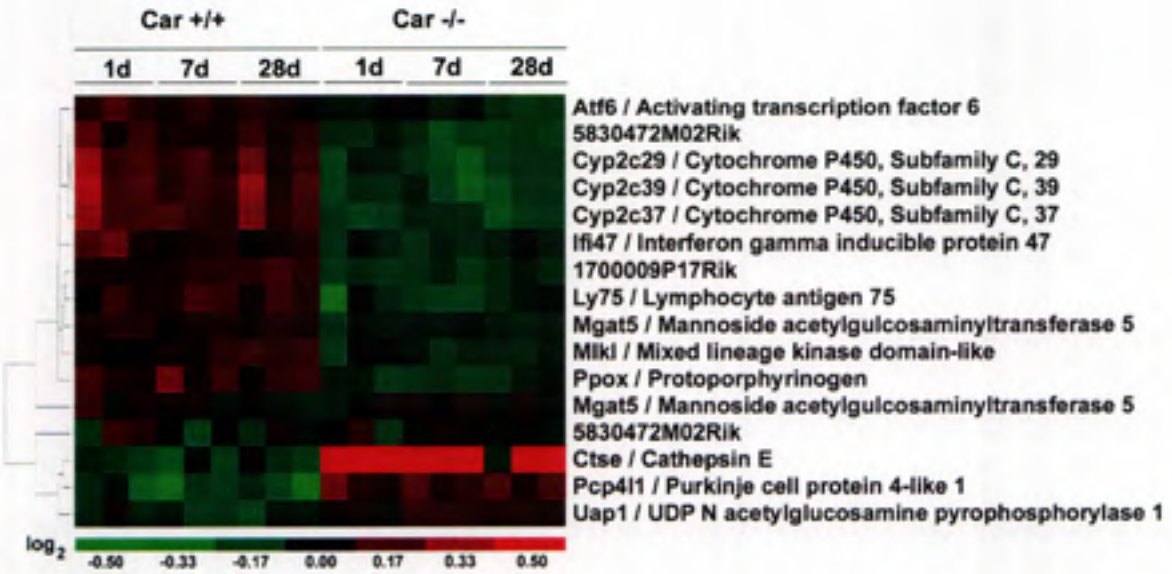

Figure 4.2. Hierarchical clustering of differentially expressed genes based on EDGE Analysis and Ingenuity Xenobiotic Metabolism Canonical Pathway. EDGE software was used to identify 1855 significant genes across time and treatment with FDR of <0.05 and P<0.05 and visualized in JavaTreeView (**A**). These genes were uploaded to Ingenuity Pathways Analysis to demonstrate temporal changes in the canonical pathway for CAR-mediated xenobiotic metabolism (**B**).

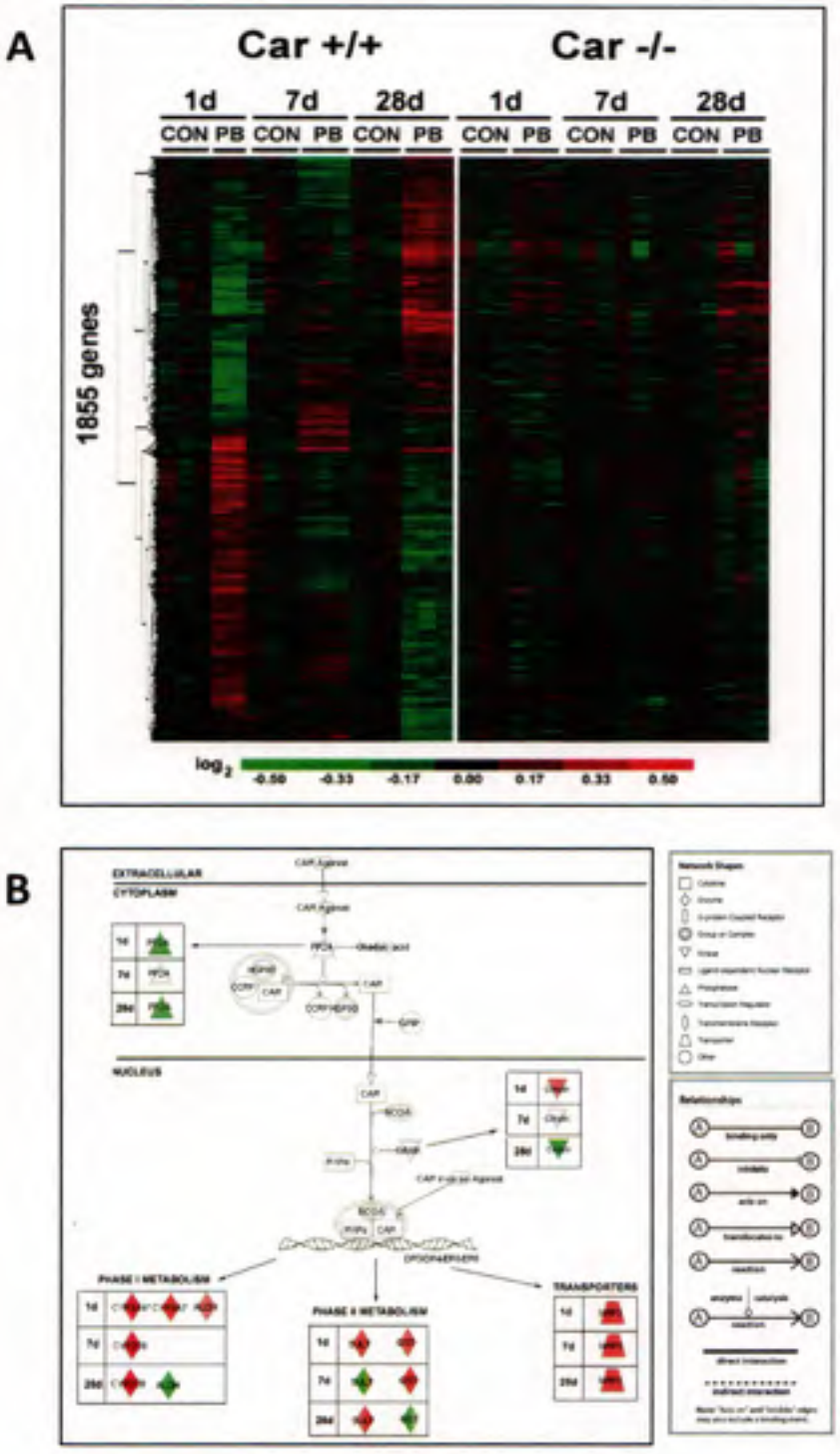

Figure 4.3. Hierarchical clustering of EDGE significant genes with DWD-adjusted PB and WY data. Distance Weighted Discrimination was used to combine PB and WY data sets in order to account for batch effects. EDGE significant genes in response to PB (1855) were extracted from the WY data set, clustered, and visualized side-by-side using JavaTreeView (**A**). By the same procedure, significant genes from WY EDGE analysis (1294) were extracted from PB data and gene-by-gene comparisons were made (**B**).

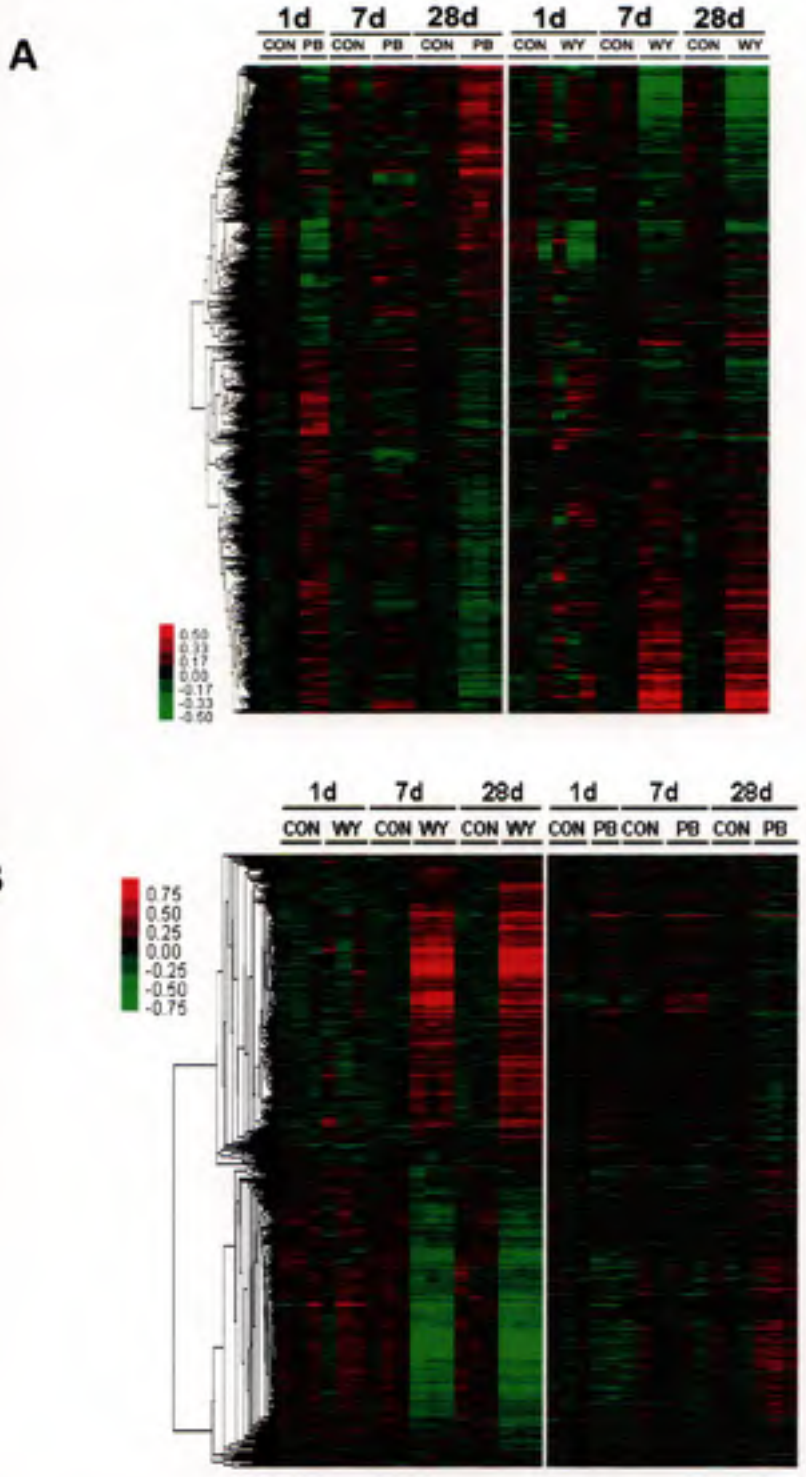

Figure 4.4. Pathway heatmap of biological processes affected by PB and/or WY-14,643 in the liver of wild-type mice. Significant gene lists from two separate EDGE analyses on PB or WY data were submitted to High-throughput GOMiner to identify significantly enriched biological pathways in response to treatment (FDR <0.05). Red or green color indicates up- or down-regulation of the biological process while intensity of color indicates a more significant False Discovery Rate.

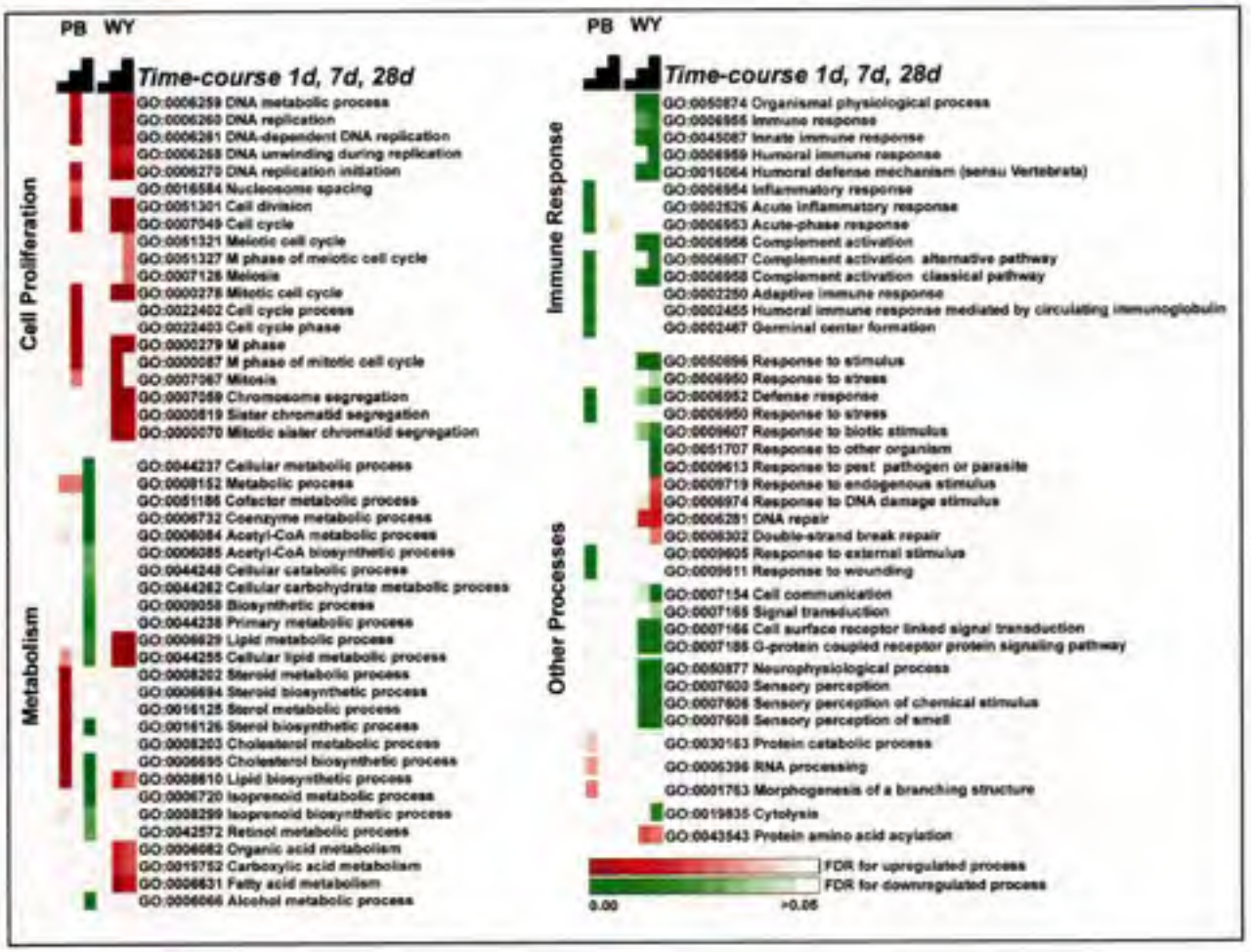

Figure 4.5. Gene networks demonstrate similar and divergent responses in response to PB or WY. DNA Replication, Recombination, and Repair, Cell Cycle, Cell Death Network generated by Ingenuity Pathways Analysis at 7d PB treatment (**A**) and 28d WY treatment (**B**). Cell Death, Organismal Injury and Abnormalities, and Cancer Network at 28d PB treatment(**C**) and 28d WY treatment (**D**).

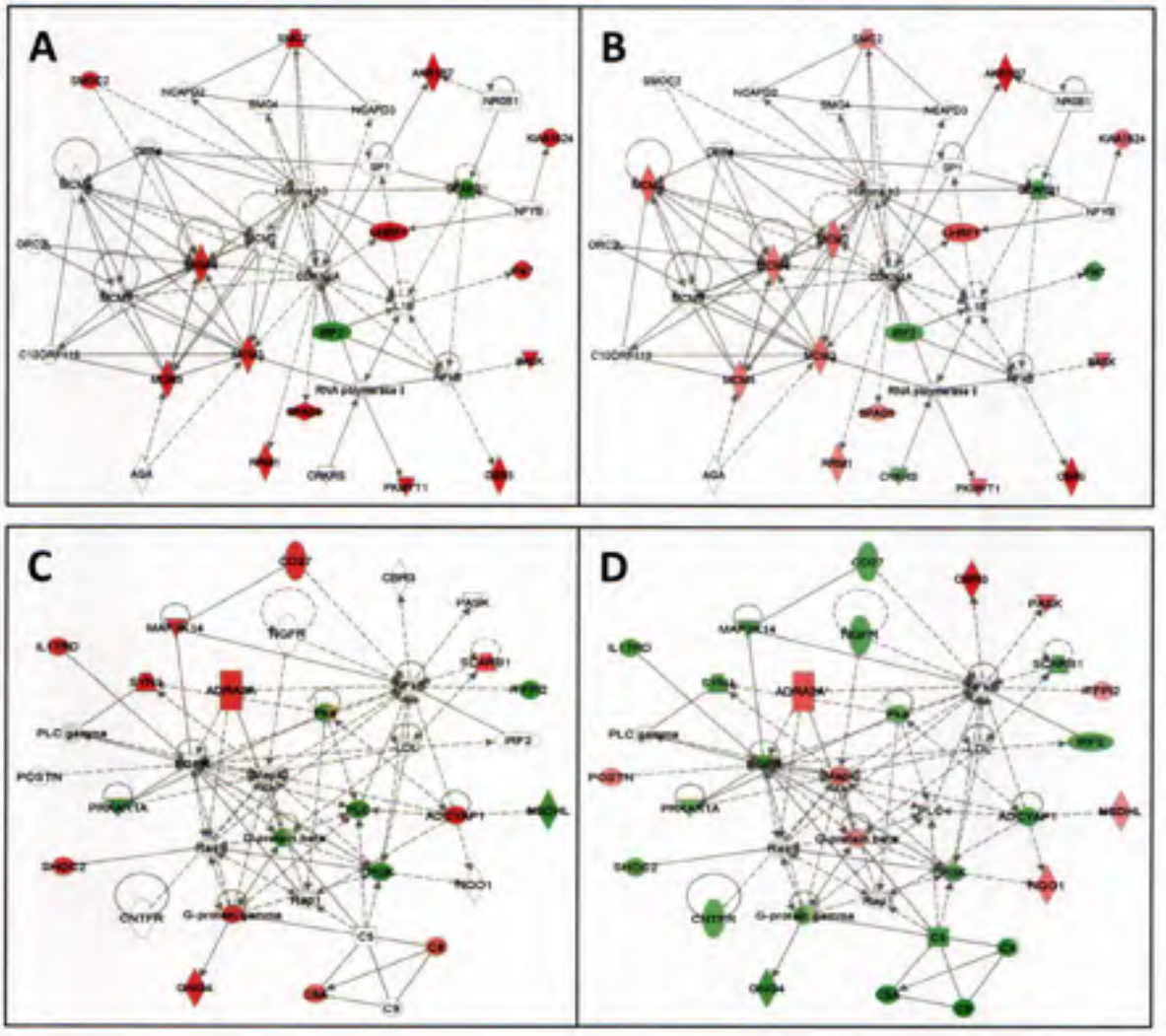

CHAPTER 5

CONCLUSIONS AND FUTURE DIRECTIONS

The goal of this study was to identify biological pathways of activated nuclear receptors over a time-course by means of gene expression profiling. We hypothesized that the initial transcriptional responses to the xenobiotic activators PB and WY-14,643 would be different because two different nuclear receptors were activated (CAR versus PPAR-alpha), but at later time-points these pathways would converge because the modes of action of the two chemicals are similar. We found that there were similarities in the cellular proliferation pathways that were activated, but the temporal activation of this response was different between PB and WY. There was divergence in general metabolism pathways and immune response, which refuted our hypothesis. The pathway mapping was important to examine general changes as opposed to changes in individual transcripts.

We also felt it was necessary to examine whether basal expression was significantly different between the wild-type and *Car*-knockout. Our results showed 14 genes that differed in basal expression. Since there was only a small subset of genes that were found to be differentially expressed, this effect was most likely negligible but still essential to identify. It was also important to demonstrate a CAR-specific signature in response to PB and the large role that CAR plays in modulating physiological responses.

In identifying these changes in gene expression, the significance of a time-course was emphasized. Previous experiments most often used a single time-point or sometimes

two time-points. The response to xenobiotics is a dynamic one and often includes transient processes, so assaying transcription at a single time-point may not be an accurate portrayal of physiological changes. The need for multiple time-points is also significant for risk assessment for genomic profiling of response to toxicants. Many researchers have tried to identify "fingerprints" of gene expression as a way to classify chemicals which have the ability to cause cancer through various mechanisms. Our studies indicate that this method of binning chemicals may not be useful because a convergence of pathway responses at later time-points was not seen.

The study is limited by the fact that PB and WY-14,643 may not act exclusively through the nuclear receptors we targeted. Furthermore, the use of a knockout model may not be a true biological model because other genes may be upregulated or downregulated in order to compensate for the absence of the target genes. This body of work could be improved by adding another treatment group for PPAR-alpha null mice on C57BL6/J background and treated with control or WY-14643 at the same time-points. Addition of this group would also be beneficial to understand genes that differed in basal expression of PPAR-alpha, although analysis of PPAR-alpha null on an mice on an SV129 genetic background produced a small set of genes that were different at basal levels (2007b).

Our present study provides a starting point for future work. First, the time-course data model is of emerging importance to determine biological changes that are temporally significant. The study design may be helpful in identifying transient changes that may have biological significance in response to a toxicologic insult. This could extend to additional time-points, doses, and cell types in order to elucidate a comprehensive response to a

specific insult. The time-course microarray data may also be useful in identifying quantitative structure activity relationships (QSAR) between a chemical and biological responses over time. Currently, only chemical descriptors are used to create models, but the use of biological descriptors from microarray studies may also prove useful in creating a more powerful and predictive QSAR model to determine toxicity. Additionally, the National Center for Computational Toxicology is currently undertaking a "virtual liver" project which would create a complex computer model to simulate the adverse effects of toxicants. Specific short term goals of the project are to: "(a) curate mechanistic knowledge about non-genotoxic cancer in rodents and humans and to formally describe the species differences; (b) develop initial dynamic models of literature-derived NR-mediated molecular interaction networks, beginning with xenobiotic metabolism; and (c) develop an initial tissue level model of the hepatic lobule representing the key cell types, their interactions, and the nutrients and xenobiotic gradient due to blood flow" (http://www.epa.gov/comptox/virtual_liver/index.html). Overall, our work aligns with these goals and would aid in this project design. These data may be useful to reduce the number of animals used in studies and could accurately determine responses to adverse toxicants which are numerous in the environment.

REFERENCES

1. Aranda, A., and Pascual, A. (2001). Nuclear hormone receptors and gene expression. Physiol Rev. **81**, 1269-1304.

2. Benito, M., Parker, J., Du, Q., Wu, J., Xiang, D., Perou, C. M., and Marron, J. S. (2004). Adjustment of systematic microarray data biases. Bioinformatics. **20**, 105-114.

3. Cheung, H. H., Arora, V., and Korneluk, R. G. (2006). Abnormalities of cell structures in tumors: apoptosis in tumors. EXS 201-221.

4. Echchgadda, I., Song, C. S., Oh, T., Ahmed, M., De, L. C., I, and Chatterjee, B. (2007). The xenobiotic-sensing nuclear receptors pregnane X receptor, constitutive androstane receptor, and orphan nuclear receptor hepatocyte nuclear factor 4alpha in the regulation of human steroid-/bile acid-sulfotransferase. Mol Endocrinol. **21**, 2099-2111.

5. Forman, B. M., Tzameli, I., Choi, H. S., Chen, J., Simha, D., Seol, W., Evans, R. M., and Moore, D. D. (1998). Androstane metabolites bind to and deactivate the nuclear receptor CAR- beta. Nature **395**, 612-615.

6. Gonzalez, F. J. (2005). Role of cytochromes P450 in chemical toxicity and oxidative stress: studies with CYP2E1. Mutat.Res **569**, 101-110.

7. Gonzalez, F. J., and Shah, Y. M. (2008). PPARalpha: Mechanism of species differences and hepatocarcinogenesis of peroxisome proliferators. Toxicology **246**, 2-8.

8. Gronemeyer, H., Gustafsson, J. A., and Laudet, V. (2004). Principles for modulation of the nuclear receptor superfamily. Nat.Rev Drug Discov. **3**, 950-964.

9. Honkakoski, P., and Negishi, M. (1998). Protein serine/threonine phosphatase inhibitors suppress phenobarbital-induced Cyp2b10 gene transcription in mouse primary hepatocytes. Biochem J **330 (Pt 2)**, 889-895.

10. International Agency for Research on Cancer. Some Thyrotropic Agents. (79), 161. 2001. World Health Organization. IARC Monogr Eval Carcinog Risks Hum.

Ref Type: Serial (Book,Monograph)

11. Jackson, J. P., Ferguson, S. S., Moore, R., Negishi, M., and Goldstein, J. A. (2004). The constitutive active/androstane receptor regulates phenytoin induction of Cyp2c29. Mol Pharmacol **65**, 1397-1404.

12. Jackson, J. P., Ferguson, S. S., Negishi, M., and Goldstein, J. A. (2006). Phenytoin induction of the cyp2c37 gene is mediated by the constitutive androstane receptor. Drug Metab Dispos **34**, 2003-2010.

13. Kakizaki, S., Karami, S., and Negishi, M. (2002). Retinoic acids repress constitutive active receptor-mediated induction by 1,4-bis[2-(3,5-dichloropyridyloxy)]benzene of the CYP2B10 gene in mouse primary hepatocytes. Drug Metab Dispos **30**, 208-211.

14. Kawamoto, T., Sueyoshi, T., Zelko, I., Moore, R., Washburn, K., and Negishi, M. (1999). Phenobarbital-responsive nuclear translocation of the receptor CAR in induction of the CYP2B gene. Mol.Cell Biol. **19**, 6318-6322.

15. Koike, C., Moore, R., and Negishi, M. (2005). Localization of the nuclear receptor CAR at the cell membrane of mouse liver. FEBS Lett **579**, 6733-6736.

16. Leek, J. T., Monsen, E., Dabney, A. R., and Storey, J. D. (2006). EDGE: extraction and analysis of differential gene expression. Bioinformatics **22**, 507-508.

17. Levine, S. L., and Perdew, G. H. (2001). Aryl hydrocarbon receptor (AhR)/AhR nuclear translocator (ARNT) activity is unaltered by phosphorylation of a periodicity/ARNT/single-minded (PAS)-region serine residue. Mol Pharmacol **59**, 557-566.

18. Maglich, J. M., Parks, D. J., Moore, L. B., Collins, J. L., Goodwin, B., Billin, A. N., Stoltz, C. A., Kliewer, S. A., Lambert, M. H., Willson, T. M., and Moore, J. T. (2003). Identification of a novel human constitutive androstane receptor (CAR) agonist and its use in the identification of CAR target genes. J Biol Chem **278**, 17277-17283.

19. Maglich, J. M., Stoltz, C. M., Goodwin, B., Hawkins-Brown, D., Moore, J. T., and Kliewer, S. A. (2002). Nuclear pregnane x receptor and constitutive androstane receptor regulate overlapping but distinct sets of genes involved in xenobiotic detoxification. Molecular Pharmacology **62**, 638-646.

20. Morimura, K., Cheung, C., Ward, J. M., Reddy, J. K., and Gonzalez, F. J. (2006). Differential susceptibility of mice humanized for peroxisome proliferator-activated receptor {alpha} to Wy-14,643-induced liver tumorigenesis. Carcinogenesis.

21. Nuclear Receptors Nomenclature Committee (1999). A unified nomenclature system for the nuclear receptor superfamily. Cell **97**, 161-163.

22. Overington, J. P., Al Lazikani, B., and Hopkins, A. L. (2006). How many drug targets are there? Nat.Rev Drug Discov. **5**, 993-996.

23. Palmer, C. N., Hsu, M. H., Griffin, K. J., Raucy, J. L., and Johnson, E. F. (1998). Peroxisome proliferator activated receptor-alpha expression in human liver. Mol.Pharmacol **53**, 14-22.

24. Peters, J. M., Cattley, R. C., and Gonzalez, F. J. (1997). Role of PPAR alpha in the mechanism of action of the nongenotoxic carcinogen and peroxisome proliferator Wy-14,643. Carcinogenesis **18**, 2029-2033.

25. Reddy, J. K., Rao, M. S., Azarnoff, D. L., and Sell, S. (1979). Mitogenic and carcinogenic effects of a hypolipidemic peroxisome proliferator, [4-chloro-6-(2,3-xylidino)-2-pyrimidinylthio]acetic acid (Wy-14, 643), in rat and mouse liver. Cancer Research **39**, 152-161.

26. Sadler, K. C., Krahn, K. N., Gaur, N. A., and Ukomadu, C. (2007). Liver growth in the embryo and during liver regeneration in zebrafish requires the cell cycle regulator, uhrf1. Proc.Natl.Acad Sci U.S.A **104**, 1570-1575.

27. Sueyoshi, T., Moore, R., Sugatani, J., Matsumura, Y., and Negishi, M. (2008). PPP1R16A, the membrane subunit of protein phosphatase 1beta, signals nuclear translocation of the nuclear receptor constitutive active/androstane receptor. Mol Pharmacol **73**, 1113-1121.

28. Tien, E. S., and Negishi, M. (2006). Nuclear receptors CAR and PXR in the regulation of hepatic metabolism. Xenobiotica **36**, 1152-1163.

29. Timsit, Y. E., and Negishi, M. (2007). CAR and PXR: the xenobiotic-sensing receptors. Steroids **72**, 231-246.

30. Tusher, V. G., Tibshirani, R., and Chu, G. (2001). Significance analysis of microarrays applied to the ionizing radiation response. Proc.Natl.Acad.Sci.U.S.A **98**, 5116-5121.

31. Tzameli, I., Pissios, P., Schuetz, E. G., and Moore, D. D. (2000). The xenobiotic compound 1,4-bis[2-(3,5-dichloropyridyloxy)]benzene is an agonist ligand for the nuclear receptor CAR. Mol.Cell Biol. **20**, 2951-2958.

32. Ueda, A., Hamadeh, H. K., Webb, H. K., Yamamoto, Y., Sueyoshi, T., Afshari, C. A., Lehmann, J. M., and Negishi, M. (2002). Diverse roles of the nuclear orphan receptor CAR in regulating hepatic genes in response to phenobarbital. Molecular Pharmacology **61**, 1-6.

33. Urquhart, B. L., Tirona, R. G., and Kim, R. B. (2007). Nuclear receptors and the regulation of drug-metabolizing enzymes and drug transporters: implications for interindividual variability in response to drugs. J Clin Pharmacol **47**, 566-578.

34. Wei, P., Zhang, J., Egan-Hafley, M., Liang, S., and Moore, D. D. (2000). The nuclear receptor CAR mediates specific xenobiotic induction of drug metabolism. Nature **407**, 920-923.

35. Woods, C. G., Heuvel, J. P., and Rusyn, I. (2007a). Genomic profiling in nuclear receptor-mediated toxicity. Toxicol Pathol **35**, 474-494.

36. Woods, C. G., Kosyk, O., Bradford, B. U., Ross, P. K., Burns, A. M., Cunningham, M. L., Qu, P., Ibrahim, J. G., and Rusyn, I. (2007b). Time course investigation of PPARalpha- and Kupffer cell-dependent effects of WY-14,643 in mouse liver using microarray gene expression. Toxicol Appl Pharmacol **225**, 267-277.

37. Yamamoto, Y., Moore, R., Goldsworthy, T. L., Negishi, M., and Maronpot, R. R. (2004). The orphan nuclear receptor constitutive active/androstane receptor is essential for liver tumor promotion by phenobarbital in mice. Cancer Res **64**, 7197-7200.

38. Yoshinari, K., Kobayashi, K., Moore, R., Kawamoto, T., and Negishi, M. (2003). Identification of the nuclear receptor CAR:HSP90 complex in mouse liver and recruitment of protein phosphatase 2A in response to phenobarbital. FEBS Lett **548**, 17-20.

39. Zeeberg, B. R., Qin, H., Narasimhan, S., Sunshine, M., Cao, H., Kane, D. W., Reimers, M., Stephens, R. M., Bryant, D., Burt, S. K., Elnekave, E., Hari, D. M., Wynn, T. A., Cunningham-Rundles, C., Stewart, D. M., Nelson, D., and Weinstein, J. N. (2005). High-Throughput GoMiner, an 'industrial-strength' integrative gene ontology tool for interpretation of multiple-microarray experiments, with application to studies of Common Variable Immune Deficiency (CVID). BMC.Bioinformatics **6**, 168.

40. Zelko, I., and Negishi, M. (2000). Phenobarbital-elicited activation of nuclear receptor CAR in induction of cytochrome P450 genes. Biochem Biophys.Res Commun. **277**, 1-6.

41. Zhang, Z., Burch, P. E., Cooney, A. J., Lanz, R. B., Pereira, F. A., Wu, J., Gibbs, R. A., Weinstock, G., and Wheeler, D. A. (2004). Genomic analysis of the nuclear receptor family: new insights into structure, regulation, and evolution from the rat genome. Genome Res **14**, 580-590.